

Article

Identifying Pseudorutile and Kleberite Using Raman Spectroscopy

Alexis Imperial ¹, Georgia Pe-Piper ^{1,*} , David J. W. Piper ² and Ian E. Grey ³¹ Department of Geology, Saint Mary's University, Halifax, NS B3H 3C3, Canada² Natural Resources Canada, Geological Survey of Canada (Atlantic), Bedford Institute of Oceanography, Dartmouth, NS B2Y 4A2, Canada³ CSIRO Mineral Resources, Private bag 10, Clayton South, VIC 3169, Australia

* Correspondence: gpiper@smu.ca

Abstract: Pseudorutile and kleberite are intermediate minerals formed during alteration of ilmenite to rutile. They are difficult to identify, as both have a range of chemical composition and occur as small crystals commonly mixed with other minerals. Reference samples of large crystals of pseudorutile and kleberite, with published X-ray diffraction and chemical analyses, were analysed to establish characteristic Raman spectra. Pseudorutile produced a goethite-like Raman spectrum but with a shift to increased wavenumber. It has characteristic Raman bands with peak positions at 234, 302, 402, 546, 617, 713 and 816 cm^{-1} and OH stretching over the interval of 3390–3350 cm^{-1} . The 402 and 806 cm^{-1} bands are the most intense. Kleberite produced a similar spectrum, but with a 10–30 cm^{-1} greater Raman shift in the goethite-like bands. Its Raman bands have peak positions at 432, 573, 740, and 820 cm^{-1} and OH stretching at 3390–3350 cm^{-1} . These results were applied to identify pseudorutile formed by diagenetic alteration of detrital ilmenite in Cretaceous sandstones of the Mesozoic Scotian Basin, eastern Canada. These samples showed pseudorutile Raman bands, but some samples are intermixed with residual ilmenite. Raman microspectroscopy thus allows rapid identification of small grains of pseudorutile and kleberite.

Keywords: pseudorutile; kleberite; Raman spectroscopy; South Australia; Indonesia; Scotian Basin

Citation: Imperial, A.; Pe-Piper, G.; Piper, D.J.W.; Grey, I.E. Identifying Pseudorutile and Kleberite Using Raman Spectroscopy. *Minerals* **2022**, *12*, 1210. <https://doi.org/10.3390/min12101210>

Academic Editor: Nikita V. Chukanov

Received: 26 August 2022

Accepted: 23 September 2022

Published: 25 September 2022

Publisher's Note: MDPI stays neutral with regard to jurisdictional claims in published maps and institutional affiliations.



Copyright: © 2022 by the authors. Licensee MDPI, Basel, Switzerland. This article is an open access article distributed under the terms and conditions of the Creative Commons Attribution (CC BY) license (<https://creativecommons.org/licenses/by/4.0/>).

1. Introduction

Pseudorutile and kleberite are both intermediate minerals that form by the alteration of ilmenite to rutile (or anatase) during weathering or diagenesis, and occur in a variety of sedimentary strata. The alteration of ilmenite involves oxidation and leaching or removal of iron in the presence of water, which results in the production of titania minerals (rutile or anatase) as a residual by-product [1,2]. Frost et al. [3] used the ratio $\text{Ti}/(\text{Ti}+\text{Fe})$ to name the mineral phases in altered grains, with ilmenite <0.5 ; pseudorutile 0.5–0.7; leucoxene 0.7–0.9; and rutile >0.9 . The presence of pseudorutile as product of ilmenite alteration has been identified in lateritic soils [4], coastal dunes [5], placer deposits [6], and in sandstones in sedimentary basins [7–9]. Kleberite has been recognized in ilmenite-bearing Cenozoic sands from Germany [10], Australia [11,12] and Indonesia [13].

Larger crystals of pseudorutile and kleberite have been identified by X-ray diffraction analysis [8,12–17] and chemical composition has also been used for identification [3,9]. The present study arose from the need to identify small diagenetic Fe-Ti minerals in deeply buried sandstones of the Mesozoic Scotian Basin, offshore eastern Canada. Thus, the first objective of this study was to use the reference samples of pseudorutile and kleberite, with published X-ray diffraction and chemical analyses, to establish characteristic Raman spectra for pseudorutile and kleberite. The second objective was to apply Raman microspectrometry to Scotian Basin sandstones to distinguish any pseudorutile or kleberite from other Fe- and Ti-rich minerals such as goethite, ilmenite, rutile and anatase. Compared to other analytical methods, Raman spectroscopy has the following advantages: (1) it provides identification of goethite, ilmenite, rutile and anatase using known Raman spectra

of the minerals available in the literature; (2) it is a non-destructive method for identifying Ti-Fe minerals; (3) it has a spatial resolution of approximately 2 microns, ideal for identifying microcrystalline pseudorutile and kleberite.

2. Review of Crystal Structure and Mineralogical Status of Pseudorutile and Kleberite

Pseudorutile is an ilmenite alteration mineral that was first introduced by Teufer and Temple [2] as a new mineral with hexagonal symmetry and an ideal composition of $\text{Fe}_2^{3+}\text{Ti}_3\text{O}_9$. However, the Commission on New Minerals and Mineral Names (CNMNC) of the International Mineralogical Association (IMA) did not accept pseudorutile as a valid mineral species. Grey and Reid [14] refined the crystal structure of pseudorutile using chemical and X-ray diffraction analyses on a single crystal of pseudorutile from Kalimantan, Indonesia. Later, Grey et al. [8] revalidated pseudorutile as a mineral species assigning Neptune Island, South Australia as the neo-type locality. Another ilmenite alteration mineral, closely related to pseudorutile, was discovered in northeast Germany and was described by Bautsch et al. [15] as kleberite, without IMA approval. Chemical and X-ray diffraction studies from heavy mineral separates collected from the Murray Basin, southeast Australia [12] and Kalimantan, Indonesia [13] had identified a very similar alteration mineral, referred to as ‘hydroxylite pseudorutile’. This mineral produced a powder X-ray diffraction pattern similar to pseudorutile but with a high content of hydroxyls. Grey et al. [16] reclassified ‘hydroxylite pseudorutile’ as kleberite and described its mineral properties using both a kleberite sample from Germany and ‘hydroxylite pseudorutile’ samples from South Australia and Indonesia. As a result, ‘hydroxylite pseudorutile’ has been accepted as a new mineral by IMA CNMNC and was officially named kleberite, after Prof. Will Kleber [17].

Although pseudorutile is often described as an oxide mineral in the literature, early Russian studies showed that ilmenite alteration involves hydration/hydroxylation as well as oxidation [18]. Later hydrothermal experimental analyses using a synthetic pseudorutile specimen also demonstrated pseudorutile as an oxyhydroxide [19]. The structure of pseudorutile is based on fine-scale intergrowth of rutile-type and goethite-type domains in a microcrystalline twinned structure similar to tivanite ($\text{V}^{3+}\text{TiO}_3\text{OH}$) [20]. The two components are: (1) rutile-type $\text{M}(1)\text{O}_2$ and (2) goethite-type $\text{M}(2)\text{O}(\text{OH})$ (Figure 1). Pseudorutile has dominant Fe^{3+} in the $\text{M}(2)$ metal-atom site rather than V^{3+} in tivanite. Kleberite is also a microcrystalline twinned analogue of tivanite-type structure, but with a dominant Ti^{4+} in the $\text{M}(2)$ metal atom site instead of Fe^{3+} in pseudorutile. Chemically, pseudorutile has higher amounts of Fe (35 wt%) and lower amounts of Ti (58 wt%) in comparison to kleberite, which has lower Fe content (11 wt%) and higher Ti content (61–69 wt%). Kleberite has three times more water content and higher contents of SiO_2 , Al_2O_3 and P_2O_5 than pseudorutile [13].

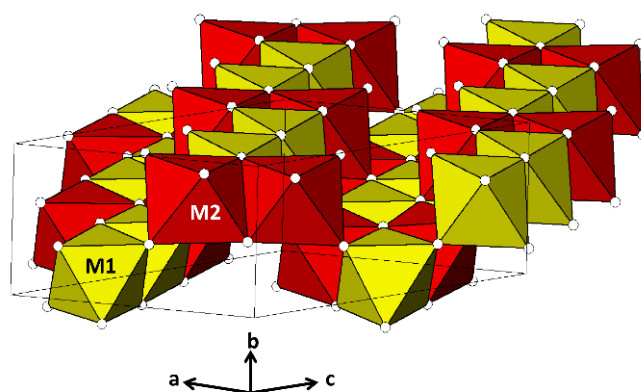


Figure 1. Polyhedral structure of pseudorutile and kleberite viewed along [101]. M1 = Ti, M2 = Fe for pseudorutile and M1 = Ti, M2 = Ti for kleberite.

3. Materials and Methods

This study used splits of samples of pseudorutile grains that had been previously identified by X-ray diffraction and chemistry. These samples were from Neptune Island, South Australia [8,12] and from Kalimantan, Indonesia [14]. Splits from previously identified samples of kleberite from Murray Basin, South Australia [16] were also analysed, to compare their Raman spectra with pseudorutile. The loose grains of South Australian pseudorutile, Indonesian pseudorutile and South Australian kleberite were provided by the Commonwealth Scientific and Industrial Research Organisation (CSIRO), Division of Mineral Resources, Australia. The loose grains were mounted and made into three separate 2.5 cm epoxy pucks, one for each locality. The pucks were made by placing compression mounting compound powder in a Buehler (Lake Bluff, IL, USA) SimpliMet 1000™ automatic mounting press with a 3-min bake time at 180 °C and 14.5 MPa, and an 11-min cool down. The grains were carefully placed on top of the powder before pressing. The pucks were then polished using diamond paste and were studied under transmitted and reflected light microscope. Five grains with a smooth and flat surface from each sample locality were chosen for this study.

The grains of pseudorutile analysed from the Scotian Basin are from polished thin sections made from heavy mineral separates of Cretaceous sandstone in the Sable Island 5H-58 well at the 1577.68 m interval. These rock samples were provided by the Canada-Nova Scotia Offshore Petroleum Board (CNSOPB) Geoscience Research Centre. Mineral grains with the chemical composition of pseudorutile [3] were chosen for this study.

All samples were analysed by laser Raman microspectroscopy (Supplementary Materials). Raman spectra were collected using a Horiba Jobin-Yvon (Burlington, ON, Canada) LabRam HR confocal instrument, at Saint Mary's University, Halifax, Canada. The equipment uses a 100 mW 532 nm Nd-YAG diode laser from Toptica Photonics (Munich, Germany) and a Synapse charge-coupled device from Horiba Jobin-Yvon. The reference objective SP-RCO-XP (Horiba Scientific; NIST traceable reference material) was used for frequency calibration. All analyses were acquired using an accumulation of three, 20 s acquisitions at 1% laser power with a 600 grooves/mm grating. The laser has a spot size of approximately 2 µm and a confocal hole diameter of 75 µm. The spectra were differentiated from other Ti-Fe minerals using known Raman spectra of ilmenite, goethite and rutile referenced from various literature and the RRUFF database [21,22]. Ilmenite has diagnostic Raman bands at 158, 220, 331, 368 and 687 cm⁻¹. Goethite produces characteristic Raman bands at 223, 240, 298, 386, 397, 477, 548 and 678 cm⁻¹, whereas rutile has Raman bands at 240, 450 and 615 cm⁻¹.

Chemical analyses of the pseudorutile grains that were investigated by Raman microspectroscopy were acquired by electron microprobe at the Regional Electron Microprobe Centre at Dalhousie University, Halifax, Canada (Table 1). All analyses were performed using JEOL (Tokyo, Japan) 8200 electron microprobe (EMP) which is equipped with Noran 133 eV dispersive spectrometer and five wavelength spectrometers (WDS). Comparison was made with previously published analyses from the same set of samples from South Australia and Indonesia [8,16]. For the Scotian Basin samples, the Ti/(Ti+Fe) ratio [3], was calculated using EMP results to distinguish Scotian Basin pseudorutile from other Ti-Fe minerals and/or mixtures such as 'leucoxene'.

In addition, all analysed samples were imaged at the Regional Analytical Centre at Saint Mary's University, Halifax, Canada. The analyses were made using a TESCAN (Warrendale, PA, USA) MIRA 3 LMU Variable Pressure Schottky Field Emission scanning electron microscope (SEM) equipped with an INCA (Oxford Instruments, High Wycombe, England) X-max 80 mm² silicon drift detector (SDD) Energy Dispersive Spectrometer (EDS) and Backscattered Electron (BSE) detector. These SEM-EDS analyses are relatively imprecise and were used only for quick confirmation of mineral identification. The BSE images were acquired for textural and morphological details of the studied grains.

Table 1. Chemical analyses of pseudorutile and kleberite.

	Pseudorutile				Kleberite		
	South Australia		Indonesia		Scotian B.	South Australia	
	This Study EMP (5 Grains) Average	(Grey and Reid (1975) [14]	This Study EMP (5 Grains) Average	(Grey and Reid (1975) [14]	This Study EMP (10 Grains) Average	This Study SEM (5 Grains) Average	(Grey et al., 2013) [16]
SiO ₂	0.2	b.d.	0.3	b.d.	0.54	1.2	1.70
TiO ₂	58.0	58.84	60.8	63.02	63.19	71.6	69.30
Al ₂ O ₃	0.2	b.d.	0.4	b.d.	0.39	1.4	2.50
FeOt	31.9	35.89	25.3	30.51	27.57	8.6	10.30
Cr ₂ O ₃	b.d.	b.d.	b.d.	b.d.	0.10	b.d.	b.d.
MgO	0.3	b.d.	b.d.	b.d.	0.09	0.4	0.46
MnO	0.7	0.6	2.8	2.87	1.12	b.d.	0.21
CaO	0.1	b.d.	b.d.	b.d.	0.03	b.d.	b.d.
Na ₂ O	b.d.	b.d.	b.d.	b.d.	0.07	0.6	b.d.
P ₂ O ₅	b.d.	b.d.	b.d.	b.d.	b.d.	0.6	0.41
ZnO	b.d.	b.d.	b.d.	b.d.	0.05	b.d.	b.d.
Nb ₂ O ₅	b.d.	b.d.	0.4	b.d.	0.06	b.d.	b.d.
BaO	b.d.	b.d.	b.d.	b.d.	0.12	b.d.	b.d.
ZrO ₂	b.d.	b.d.	b.d.	b.d.	0.02	b.d.	b.d.
V ₂ O ₅	b.d.	b.d.	b.d.	b.d.	0.07	1.2	0.30
H ₂ O	n.d.	3.24	n.d.	2.08	n.d.	n.d.	10.90
Total	91.6	98.57	90.1	98.48	93.42	84.0	96.10

n.d.—not determined. b.d.—below detection limit or not reported. SEM EDS chemical analyses normalized to 84%, to compensate for undetected light elements. Reported FeO, Fe₂O₃ or (FeO+Fe₂O₃) are all recalculated as FeOt.

4. Results

4.1. Pseudorutile

The acquired Raman spectra of South Australian and Indonesian pseudorutile over the interval 0 to 1200 cm⁻¹ are very similar (Figures 2 and 3). The spectra are consistent with pseudorutile consisting of a microcrystalline twinned tivanite-type structure involving goethite and rutile domains [20]. We suggest that there are independent (or almost independent) vibrations of the goethite-type and rutile-type domains, resulting in a goethite-like band (3E_g + 2A_{1g}) and a rutile-like band (A_{1g} + B_{1g} + B_{2g} + E_g) with a complete symmetry of B_{1g} + B_{2g} + 4E_g + 3A_{1g}, with four active modes (B_{1g} + 2E_g + A_{1g}). Eight bands were assigned with reference to known vibrational modes of both goethite and rutile (Table 2). O-H asymmetric stretching vibration was identified around 3390–3550 cm⁻¹. The majority of the spectral peaks that resemble goethite bands in spectra of both South Australian and Indonesian samples (bands 1, 2, 3, 6 and 7–8 in Figures 2 and 3) appear to be shifted to higher wavenumber than those reported in the literature for goethite [23]. Bands 1 and 4 have a maximum shift of around 11 cm⁻¹. The peak assigned to Fe-OH asymmetric stretch at 477 cm⁻¹ (band 4) was only present in one sample, Ind-1. Bands 2 and 5 have a shift to higher wavenumber of up to 22 cm⁻¹. Bands 3 and 7 have maximum shifts of 32 cm⁻¹ and 42 cm⁻¹, respectively. The peak assigned to the Ti-O band shows no significant change from rutile reported in the literature [24].

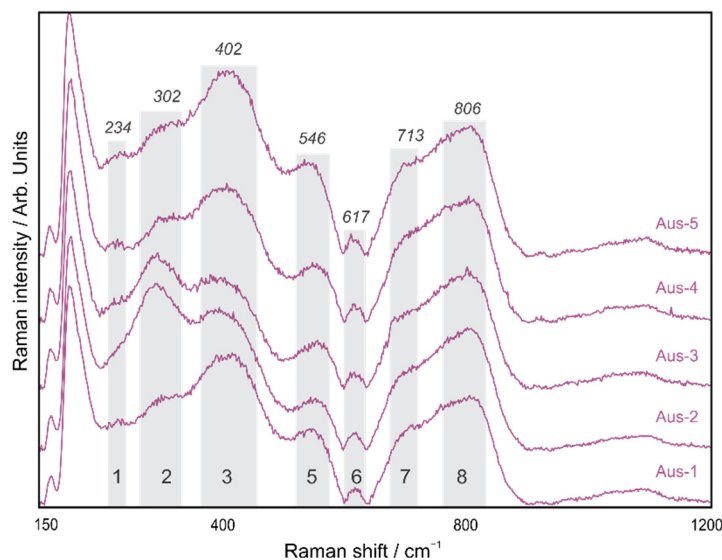


Figure 2. Raman spectra of South Australian pseudorutile showing assigned pseudorutile bands (Table 2).

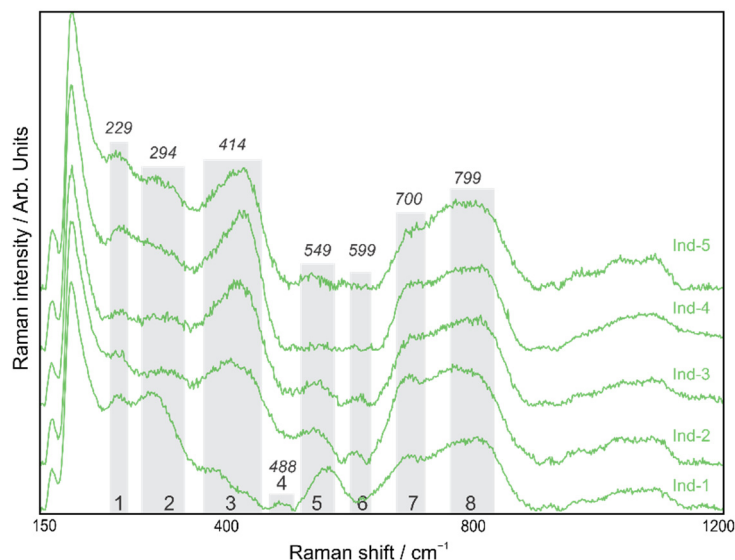


Figure 3. Raman spectra of Indonesian pseudorutile showing assigned pseudorutile bands (Table 2).

Table 2. Assignment of Raman peaks for pseudorutile and kleberite (average values in cm^{-1}).

Band no.	Goethite and *Rutile		Pseudorutile				Kleberite
	[23,24]		This Study				
			S. Austr.	Indonesia	Scotian B.	S. Austr.	
1	A _{1g}	Fe-O sym str	223	234	229	220	-
2	E _g	Fe-OH sym bend	298	302	294	290	-
3	E _g	Fe-O-Fe/-OH sym str	397	402	414	412	432
4	A _{1g}	Fe-OH asym str	477	-	488	480	-
5	-	Fe-OH asym str	548	546	549	537	573
6	*A _{1g}	*Ti-O	*615	617	599	610	-
7	-	Fe-O sym str	678	713	700	700	740
8	-	-	-	806	799	810	820

Raman spectra from grains from the Scotian Basin (Figure 4), tentatively identified as pseudorutile on the basis of chemical composition, also display goethite-like and rutile-like Raman bands that resemble the bands in South Australian and Indonesian pseudorutile

(Table 2). Many spectra also include a strong ilmenite band (Figure 4). Most of the analysed Scotian Basin grains thus appear to be mixtures of pseudorutile and ilmenite, so that the Ti/(Ti+Fe) calculations [3] may not accurately represent pseudorutile. Nevertheless, analyses ordered by Ti/(Ti+Fe) ratio in Figure 4 show systematic variation in Raman band intensity with increasing total Ti/(Ti+Fe).

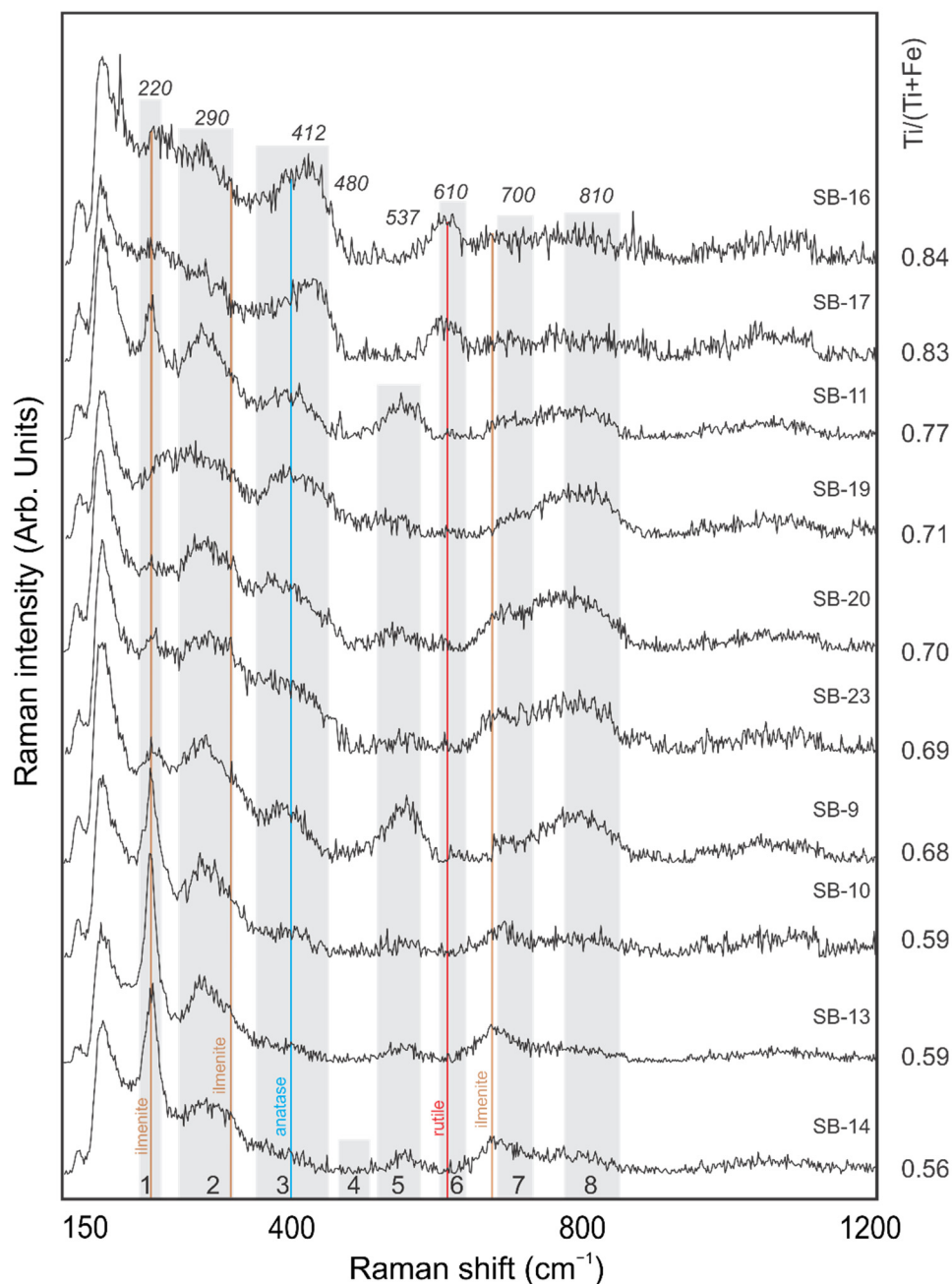


Figure 4. Raman spectra of Scotian Basin pseudorutile arranged based on increasing Ti/(Ti+Fe). Additionally, shows principal bands for ilmenite, anatase and rutile.

4.2. Kleberite

Raman spectra of kleberite over the interval 150 to 1200 cm^{-1} were compared to the spectra of both South Australian and Indonesian pseudorutile (Figure 5). Although pseudorutile and kleberite have similar structures with components of goethite and rutile, only five peaks were recognised rather than nine peaks observed for pseudorutile. Peaks were assigned with reference to both known goethite and rutile peaks, and the assigned pseu-

gorutile peaks from above (Table 2). O-H stretching is observed around 3390–3550 cm^{-1} and appears to be more noticeable in kleberite samples compared to pseudorutile samples. The kleberite spectra also display goethite-like Raman bands that are shifted to greater wavenumber, similar to pseudorutile. Assigned peak positions at the Fe-O-Fe/-OH symmetric stretch (band 1), Fe-OH asymmetric stretch (band 2), and Fe-O symmetric stretch (bands 3–4) displayed a Raman shift increase of approximately 30–35 cm^{-1} compared to known goethite peaks, and displayed a shift increase of 21–28 cm^{-1} compared to pseudorutile.

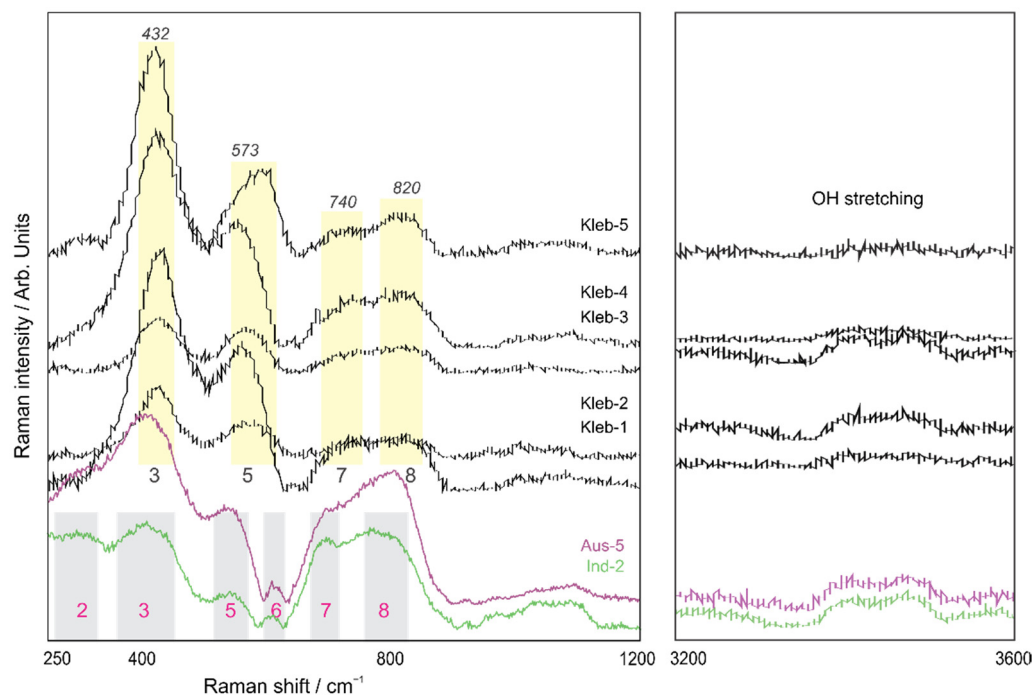


Figure 5. Raman spectrum of kleberite (black) compared to the Raman spectra of South Australian (magenta) and Indonesian (green) pseudorutile.

5. Discussion

The observed Raman shifts from the South Australian and Indonesian samples in the goethite-like bands may be due to the substitution of Ti for Fe^{3+} in the goethite-like regions of the pseudorutile structure. A similar study of well-documented shift of vibrational frequencies due to the substitution of Al into goethite showed similar band-shifting to higher wavenumbers [25]. The broadening of band 7 to 8, at 700 to 813 cm^{-1} , may also be due to the substitution of Ti in the Fe^{3+} in the Fe-O symmetric stretching of the goethite-like band, as peak broadening can also be a result of element substitution [25]. Another consideration is that both pseudorutile samples from South Australia and Indonesia are nanocrystalline [13] and powder X-ray diffraction peak widths for the South Australian pseudorutile determined that the anion lattice ordering is confined to regions of about 15 nanometres, and the ordering of the metal atoms (Fe and Ti) is limited to only a few nanometres [12]. This nanophase character can have a significant effect on the width, intensity and position of the Raman spectra peaks, compared with more crystalline samples [26].

The Indonesian pseudorutile spectra appear noisier compared to South Australian spectra (Figures 2 and 3). This may be due to the impurities present in Indonesian pseudorutile grains. Previous X-ray diffraction studies showed Indonesian pseudorutile grains to have weak diffraction lines from rutile and ilmenite [14], whereas South Australian grains were shown to be pure with no reflections of ilmenite and rutile by X-ray diffraction analyses [8]. Thus, the South Australian pseudorutile produces more consistent and clean spectra compared to Indonesian pseudorutile grains.

The increasing Raman shift in the goethite-like bands from pseudorutile to kleberite (Figure 4) is probably due to the increase of Ti in the structure. Chemically, kleberite contain higher content of Ti and lower content of Fe compared to pseudorutile (Table 1). This suggests that higher amount of Ti in kleberite, which resulted in more substitution of Ti in Fe³⁺ goethite-like region in the kleberite crystal structure, resulted in a greater shift in the Raman wavenumber. Chemical analyses of kleberite shows 81–88 wt% Ti, whereas pseudorutile shows a range of 63–73 wt% Ti, with an average 16 wt% Ti difference (Table 1). The Ti substitution may also account to additional broadening of the spectra, which masked the rutile Raman band, causing it to be completely inactive. On the other hand, the Scotian Basin pseudorutile shows changes in band intensity with Ti content, but the only systematic band shift is that the shift of band 3 diminishes with increasing Ti.

6. Conclusions

The Raman spectrum of pseudorutile includes both goethite-like bands and rutile-like bands. Pseudorutile can be easily distinguished from other Fe-Ti oxide minerals by using peak positions at 234, 302, 402, 546, 617, 713 and 816 cm⁻¹ and OH stretching from 3390–3350 cm⁻¹. The shift to higher wavenumber in the goethite-like bands, compared to pure goethite, is due to the substitution of Ti for Fe³⁺. The broadening of the spectra is mainly due to the crystal size effect. Pseudorutile samples from Indonesia and South Australia are nanocrystalline, which affects the width, intensity and even the position of the Raman spectra peaks. Kleberite has a diagnostic Raman spectrum with peak positions at 432, 573, 740 and 820 cm⁻¹. O-H stretching is present at 3390–3350 cm⁻¹. Kleberite clearly shows that the increase in the Raman shift in the goethite-like bands is due to the substitution of Ti in the Fe site.

Supplementary Materials: The following supporting information can be downloaded at: <https://www.mdpi.com/article/10.3390/min12101210/s1>, File S1: Raman spectra and backscattered electron images.

Author Contributions: Conceptualization, A.I. and G.P.-P.; Methodology, A.I.; Software, A.I.; Validation; I.E.G.; Writing—original draft preparation, A.I.; Writing—review and editing, I.E.G., G.P.-P. and D.J.W.P.; Visualization, A.I.; Supervision, G.P.-P. and D.J.W.P.; Project Administration, A.I. and G.P.-P.; Funding Acquisition, G.P.-P. All authors have read and agreed to the published version of the manuscript.

Funding: The funding for this study was provided by the Nova Scotia Offshore Energy Research Association (OERA), grant 400-191.

Data Availability Statement: Data are provided in Supplementary Materials.

Acknowledgments: We thank Mitch Kerr, Xiang Yang and Dan Macdonald for their technical assistance with Raman spectroscopy, scanning electron microscope and electron microprobe, respectively. We also thank the Academic Editor for much constructive advice.

Conflicts of Interest: The authors declare no conflict of interest. The funders had no role in the design of the study; in the collection, analyses, or interpretation of data; in the writing of the manuscript; or in the decision to publish the results.

References

1. Temple, A.K. Alteration of ilmenite. *Econ. Geol.* **1966**, *61*, 695–714. [[CrossRef](#)]
2. Teufer, G.; Temple, A.K. Pseudorutile—a new mineral intermediate between ilmenite and rutile in the alteration of ilmenite. *Nature* **1996**, *211*, 179–181. [[CrossRef](#)]
3. Frost, M.T.; Grey, I.E.; Harrowfield, I.R.; Mason, K. The dependence of alumina and silica contents on the extent of alteration of weathered ilmenites from western Australia. *Mineral. Mag.* **1983**, *47*, 201–208. [[CrossRef](#)]
4. Anand, R.R.; Gilkes, R.J. Weathering of ilmenite in a lateritic pallid zone. *Clays Clay Miner.* **1984**, *32*, 363–374. [[CrossRef](#)]
5. Puffer, J.H.; Cousminer, H.L. Factors controlling the accumulation of titanium-iron oxide-rich sands in the Cohansy Formation, Lakehurst Area, New Jersey. *Econ. Geol.* **1982**, *77*, 377–391. [[CrossRef](#)]
6. Schulz, B.; Haser, S. The ilmenite-pseudorutile-leucosene alteration sequence in placer deposits in the view of automated SEM mineral liberation analysis. *GeoBerlin* **2015**, *2015*, 336.

7. Morad, S.; Aldahan, A.A. Alteration of detrital Fe-Ti oxides in sedimentary rocks. *Geol. Soc. Am. Bull.* **1986**, *97*, 567–578. [[CrossRef](#)]
8. Grey, I.E.; Watts, J.A.; Bayliss, P. Mineralogical nomenclature: Pseudorutile revalidated and neotype given. *Mineral. Mag.* **1994**, *58*, 597–600. [[CrossRef](#)]
9. Pe-Piper, G.; Piper, D.J.W.; Dolansky, L. Alteration of ilmenite in the Cretaceous sandstones of Nova Scotia, southeastern Canada. *Clays Clay Miner.* **2005**, *53*, 490–510. [[CrossRef](#)]
10. Steinike, K. Der Kleberit im nordöstlichen Teil Deutschlands (1949–1990 Staatsgebiet der DDR). *Geohistorische Blätter* **2008**, *11*, 121–128.
11. Pownceby, M.I. Alteration and associated impurity element enrichment in detrital ilmenites from the Murray Basin, southeast Australia: A product of multistage alteration. *Aust. J. Earth Sci.* **2010**, *52*, 243–258. [[CrossRef](#)]
12. Grey, I.E.; Li, C. Hydroxylated pseudorutile derived from microilmenite in the Murray Basin, southeastern Australia. *Mineral. Mag.* **2003**, *67*, 733–747. [[CrossRef](#)]
13. Grey, I.E.; Bordet, P.; Wilson, N.C.; Townend, R.; Bastow, T.J.; Brunelli, M. A new Al-rich hydroxylated pseudorutile from Kalimantan, Indonesia. *Am. Mineral.* **2010**, *95*, 161–170. [[CrossRef](#)]
14. Grey, I.E.; Reid, A.F. The structure of pseudorutile and its role in the natural alteration of ilmenite. *Am. Mineral.* **1975**, *60*, 898–906.
15. Bautsch, H.J.; Rohde, G.; Sedlacek, P.; Zedler, A. Kleberit-Ein neues Eisen-Titan-Oxidmineral aus Tertiären Sanden. *Z. für Geol. Wiss.* **1978**, *6*, 661–671.
16. Grey, I.E.; Steinike, K.; MacRae, C.M. Kleberite, $\text{Fe}^{3+}\text{Ti}_6\text{O}_{11}(\text{OH})_5$, a new ilmenite alteration product, from Königshain, northeast Germany. *Mineral. Mag.* **2013**, *77*, 45–55. [[CrossRef](#)]
17. Warr, L.N. IMA–CNMNC approved mineral symbols. *Mineral. Mag.* **2021**, *85*, 291–320. [[CrossRef](#)]
18. Dyadchenko, M.G.; Khatuntseva, A.Y. Mineralogy and petrology of the weathering process in ilmenite. *Dokl. Akad. Nauk. SSSR* **1960**, *132*, 435–458.
19. Grey, I.E.; Li, C.; Watts, J.A. Hydrothermal synthesis of goethite-rutile intergrowth structures and their relationship to pseudorutile. *Am. Mineral.* **1983**, *68*, 981–988.
20. Grey, I.E.; Nickel, E.H. Tivanite, a new oxyhydroxide mineral from Western Australia, and its structural relationship to rutile and diasporite. *Am. Mineral.* **1981**, *66*, 866–871.
21. RRUFF Database. Available online: http://rruff.info/about/about_general.php (accessed on 4 September 2022).
22. Lafuente, B.; Downs, R.T.; Yang, H.; Stone, N. The power of databases: The RRUFF project. In *Highlights in Mineralogical Crystallography*; Armbruster, T., Danisi, R.M., Eds.; W. De Gruyter: Berlin, Germany, 2015; pp. 1–30.
23. RRUFF Database: Goethite; RRUFF IDs R050142.3, R120086, X050093, X050091. Available online: <https://rruff.info/goethite/display=default/> (accessed on 4 September 2022).
24. RRUFF Database: Rutile; RRUFF IDs R040049.3, R050031.3, R050417.3. Available online: <https://rruff.info/rutile/display=default/> (accessed on 4 September 2022).
25. Blanch, A.J.; Quinton, J.S.; Lenehan, C.E.; Pring, A. The crystal chemistry of Al-bearing goethites: An infrared spectroscopic study. *Mineral. Mag.* **2008**, *72*, 1043–1056. [[CrossRef](#)]
26. Sklute, E.C.; Kashyap, S.; Dyar, M.D.; Holden, J.F.; Tague, T.; Wang, P.; Jaret, S.J. Spectral and morphological characteristics of synthetic nanophase iron (oxyhydr)oxides. *Phys Chem Miner.* **2018**, *45*, 1–26. [[CrossRef](#)] [[PubMed](#)]